International Journal of Applied Power Engineering (IJAPE)
Vol. 15, No. 2, June 2026, pp. 712~723
ISSN: 2252-8792, DOI: 10.11591/ijape.v15.i2.pp712-723

Sliding mode control of a solar powered switched-inductor based quadratic DC-DC converter for sustainable EV battery charging application

Jawahar Marimuthu, Edward Rajan Samuel Nadar
Department of Electrical and Electronics Engineering, Mepco Schlenk Engineering College, Sivakasi, India

Article Info

Article history:

Received Jul 5, 2025
Revised Feb 10, 2026
Accepted Mar 12, 2026

Keywords:

Fast EV charging
High voltage gain
Sliding mode control
Solar electric vehicles
Switched-inductor quadratic converter

ABSTRACT

The growing demand for sustainable transportation and fast charging solutions requires efficient power conversion technologies for solar electric vehicles or electric vehicles (SEVs/EVs). A non-isolated solar-powered switched-inductor quadratic DC-DC converter is proposed here to achieve high voltage gain in a practical way under reduced stress on power devices. A switched-inductor network blended with CCM operation avoids the extremely high duty cycles and high electromagnetic interference in conventional boost converters. A sliding mode control (SMC) strategy is applied here to improve robustness against parameter variations, ensure stable operation against dynamic load variations, and extract maximum power during solar-powered charging operation. This makes the topological platform proposed in this study especially suitable for a wide variety of applications, such as for SEVs and fast-charging applications of EVs. Detailed MATLAB/Simulink analyses along with a laboratory-scale prototype verify the performance of the converter under practical operation conditions and confirm the high efficiency of 91-96% at varied irradiance, low voltage ripple of 0.5-1.5% of output voltage and input current ripple of 5-12% of input current, reduced switching losses of 1-4%, and suitability of the presented converter for renewable-energy-based transportation systems.

Corresponding Author:

Jawahar Marimuthu
Department of Electrical and Electronics Engineering, Mepco Schlenk Engineering College
Sivakasi, India
Email: jawahar.m@mepcoeng.ac.in

1. INTRODUCTION

In recent years, the number of electric vehicles (EVs) has increased significantly, primarily due to their increased efficiency and range [1]-[5]. Over the years, it is anticipated that there will be over 250 million EVs worldwide [6]. High-gain DC-DC converters, which are crucial for managing the varying voltage requirements of EV components and renewable energy systems, are a major part of this advancement [7]-[10]. Most DC-DC converters merely pass power and energy in a single direction, e.g., absorbing the energy on the motor controls or supplying the load on the source [11]. Conventional DC/DC converters, particularly step-up converters, often face limitations in achieving high voltage gain without compromising efficiency [12], [13]. These are more evident in the applications where small, economical, and dependable solutions of energy conversion are needed [14]. Furthermore, advanced techniques like sliding mode control (SMC) have been used in the control of the bidirectional converter of EV chargers to address these challenges [15].

Past research has investigated a number of methods of control to great effect, but with significant shortcomings. Mohammed *et al.* [16] applied a fuzzy logic controller-SMC (FLC-SMC) to minimize the

overshoot, but it complicated the control. Mazumdar *et al.* [17] used a genetic algorithm-based SMC (GA-SMC) in photovoltaic (PV) optimization, but it was computationally demanding. Huang *et al.* [18] proposed SMC on a boost converter, but with low voltage gain. Particle swarm optimization (PSO-SMC) was also employed by Mathew and Abraham [19], but required much tuning. Rahme *et al.* [20] suggested adaptive SMC but had no consistent performance with rapid load variations. Valedsaravi *et al.* [21] created a digital SMC to charge EVs in a fast manner, but using complex hardware. Falehi [22] presented the chattering-free binomial hyperbolic sliding mode controller (CFBHSMC), which was optimized by MOSFSA and has low tracking accuracy and sluggish convergence in PEMFC-based DC-DC boost converter management. Falehi and Salary [23] suggested the large-gain multi-stage non-isolated step-up converter (HGNISUC), but it has low efficiency, large current ripple, low voltage gain, and an unstable DC output. A fractional-order SMC (FOSMC) was proposed by Falehi [24] to efficiently regulate the reactive power and active with increased computational complexity. A robust perturbation observer-based fractional order sliding mode controller (RPO-FOSMC) was proposed by Falehi [25] to improve power extraction with fractional control's high computational complexity. To fill this gap, this study suggests a sliding mode control-based non-isolated switched inductor quadratic (SMC-NSIQ) DC-DC converter that is a hybrid of a robust nonlinear control approach and a simplified switched inductor topology. The proposed method is ideal for charging electric vehicles and applications involving renewable energy since it seeks to improve efficiency while achieving significant voltage gain. A sliding mode control strategy is implemented to enhance system robustness against parameter variations to ensure stable and efficient operation under varying load conditions and optimize power extraction in renewable charging scenarios. Figure 1 shows the configuration of a solar electric vehicle (SEV).

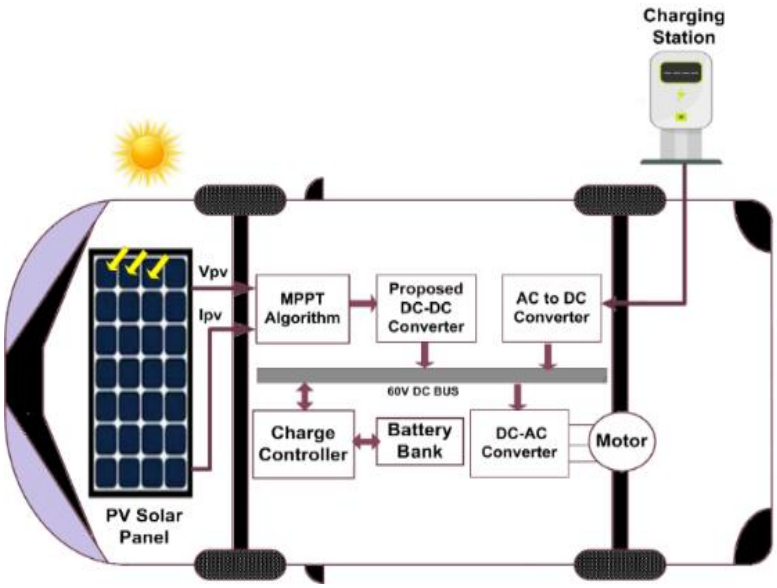

Figure 1. Configuration of solar electric vehicle

2. PROPOSED SMC – SIBQ DC-DC CONVERTER

The structure of the proposed sliding mode controlled high-gain switched-inductor based quadratic (SIBQ) DC–DC Converter is presented in Figure 2. The converter includes two active switches S_1 and S_2, three inductors L_1, L_2, and L_3, three capacitors C_1, C_2 and C_3, and six diodes D1–D6. A resistive load Rload is considered. A Switched-Inductor cell is used for increasing the voltage gain without relying on very extreme duty cycles. The converter operates at a moderate duty ratio of D=0.382, and both switches are driven synchronously, which reduces the complexity of gate drive circuits. In the proposed SIBQ converter, analytical expressions are obtained for CCM under steady state. All circuit components are considered ideal while deriving analytical expressions.

i) Mode I *(0 < t < DT):* Switches S_1 and S_2 are ON. Diodes D_1 and D_3 are forward-biased, while the remaining diodes are reverse-biased. Inductors L_1 and L_2 are charged directly from the input through D_1 and D_3. Inductor L_3 is charged by capacitors C_1 and C_2. Output capacitor C_3 supplies the load.

$$v_{L_1} = v_{in} \quad (1)$$

$$v_{L_2} = v_{in} \quad (2)$$

$$v_{L_3} = v_{C_1} + v_{C_2} \quad (3)$$

$$I_{in} = I_{L_1} + I_{L_2} \quad (4)$$

$$I_{L_1} = I_{L_2} \quad (5)$$

$$I_{C_1} = I_{C_2} = I_{L_3} \quad (6)$$

$$I_{C_3} = I_0 \quad (7)$$

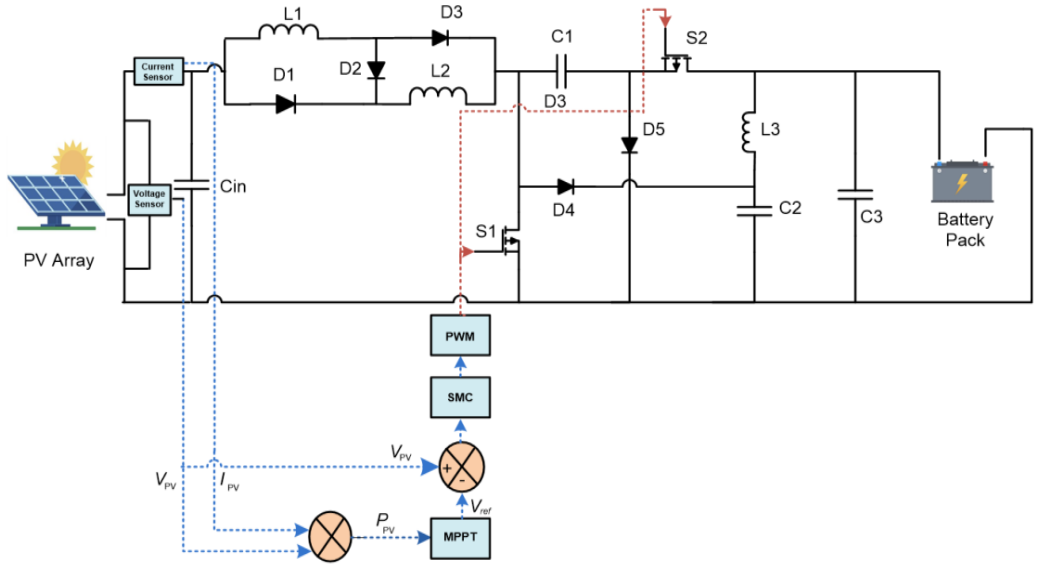

Figure 2. Proposed SMC- SIBQ DC-DC converter

ii) Mode II *(DT < t < T):* Switches S_1 and S_2 are OFF. Diodes D_2, D_4, D_5, and D_6 conduct, while D_1 and D_3 are reverse-biased. Inductors L_1 and L_2 now discharge in series with the input source. Their stored energy is transferred through diodes D_2 and D_5. Inductor L_3 delivers its stored energy to the output via diode D_6. Capacitor C_3 gets recharged.

$$v_{in} - v_{L_1} - v_{L_2} - v_{C_1} = 0 \quad (8)$$

$$v_{L_1} - v_{L_2} - v_{C_2} = 0 \quad (9)$$

$$v_{in} - v_{L_3} - v_{C_3} = 0 \quad (10)$$

$$I_{in} = I_{L_1} = I_{L_2} \quad (11)$$

$$I_{in} = I_{C_1} + I_{C_2} + I_{L_3} \quad (12)$$

$$I_{C_1} = I_{C_2} \quad (13)$$

$$I_{C_1} = I_{C_2} = \frac{I_{in} - I_{L_3}}{2} \quad (14)$$

Applying volt–second balance on the inductors using Modes 1 and 2 equations yields the DC voltage gain:

$$\frac{v_0}{v_{in}} = \left(\frac{1+D}{1-D}\right)^2 \quad (15)$$

The switching characteristics of the proposed converter is shown in Figure 3.

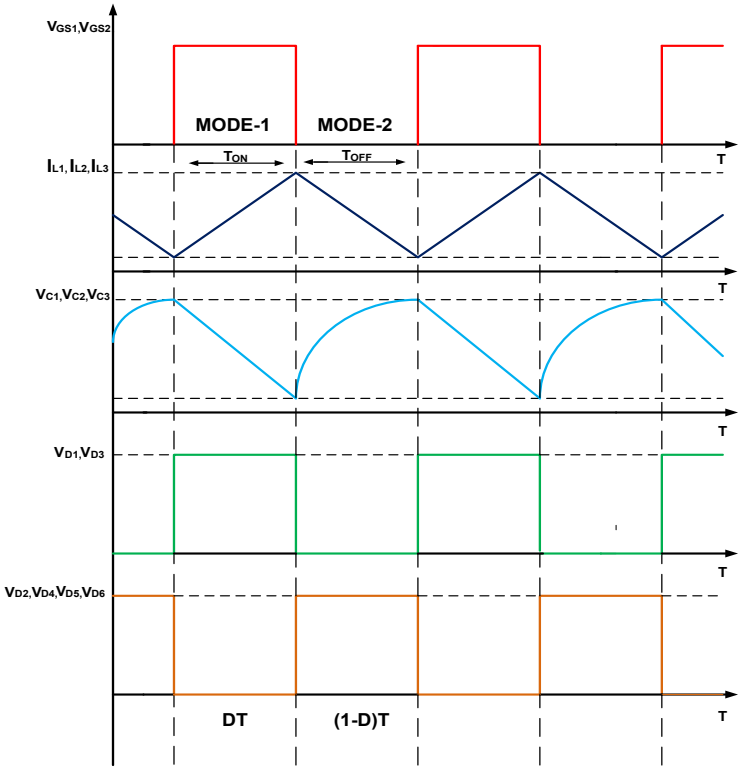

Figure 3. Voltage and current waveform in CCM

3. MATHEMATICAL MODELLING OF THE PROPOSED SMC – SIBQ DC-DC CONVERTER

The generalized state-space averaged model of a DC–DC converter is a model of its dynamic behavior over one complete switching period. Because the converter operates in two different time intervals, Mode 1 (switch ON) and Mode 2 (switch OFF), each mode will have its own state-space matrices M_1, N_1, O_1, P_1, and M_2, N_2, O_2, P_2.

$$\frac{dx(t)}{dt} = Mx(t) + Nu(t)\,; \quad y(t) = Ox(t) + Pu(t)$$

Where $M = M_1 d + M_2(1-d)$, $N = N_1 d + N_2(1-d)$, $O = O_1 d + O_2(1-d)$, $P = P_1 d + P_2(1-d)$, d is the duty cycle. As per Mode 1 and Mode 2 operations, the averaged state-space equations of the proposed quadratic boost converter are given in (16) and (17). The state equation of the proposed SMC – SIBQ DC-DC converter is given by (16).

$$\begin{bmatrix} \frac{di_{L_1}}{dt} \\ \frac{di_{L_2}}{dt} \\ \frac{di_{L_3}}{dt} \\ \frac{dv_{c_1}}{dt} \\ \frac{dv_{c_2}}{dt} \\ \frac{dv_{c_3}}{dt} \end{bmatrix} = \begin{bmatrix} 0 & 0 & 0 & \frac{(D-1)}{2L_1} & 0 & 0 \\ 0 & 0 & 0 & \frac{(D-1)}{2L_2} & 0 & 0 \\ 0 & 0 & 0 & \frac{D}{L_3} & \frac{D}{L_3} & \frac{(D-1)}{L_3} \\ 0 & 0 & \frac{(3D-1)}{2C_1} & 0 & 0 & 0 \\ 0 & 0 & \frac{(3D-1)}{2C_1} & 0 & 0 & 0 \\ 0 & 0 & 0 & 0 & 0 & \frac{(d-2)}{R_0 C_0} \end{bmatrix} \begin{bmatrix} I_{L_1} \\ I_{L_2} \\ I_{L_3} \\ V_{c_1} \\ V_{c_2} \\ V_{c_3} \end{bmatrix} + \begin{bmatrix} \frac{(1-D)}{2L_1} & 0 \\ \frac{(1-D)}{2L_2} & 0 \\ \frac{(1-D)}{L_3} & 0 \\ 0 & \frac{(1-D)}{2C_1} \\ 0 & \frac{(1-D)}{2C_2} \\ 0 & 0 \end{bmatrix} \begin{bmatrix} V_{in} & I_{in} \end{bmatrix} \quad (16)$$

The output equation of the proposed SMC – SIBQ DC-DC converter is (17).

$$V_0 = [0 \quad 0 \quad 0 \quad 0 \quad 0 \quad 1] \begin{bmatrix} I_{L_1} \\ I_{L_2} \\ I_{L_3} \\ v_{c_1} \\ v_{c_2} \\ v_{c_0} \end{bmatrix} \tag{17}$$

4. DESIGN AND SELECTION OF PASSIVE COMPONENTS

The selection of the circuit components depends on the working conditions of the converter. The required operating conditions of the converter are 12 V for the input voltage, 60 V output voltage, a switching frequency of 20 kHz, and an output power of 60 W. Based on the output conditions of the converter, the calculated duty ratio of the converter is 0.382, and hence the selection of circuit components for the operating conditions discussed above is given below.

4.1. Selection of magnetic component

To ensure the overall reliability of the power converter and to minimize size and weight constraints, ripple current is controlled through appropriate inductor design. To operate the proposed converter in continuous conduction mode, the value of inductance is selected based on input voltage (v_{in}), ripple current (ΔI_L), switching frequency (f_s), and duty ratio (D). The value of inductance is obtained by using (18) and (19).

$$L_1 = L_2 = \frac{v_{in} D}{\Delta I_L f_s} \tag{18}$$

$$L_3 = \frac{2(1+D)V_{in} D}{(1-D)\Delta I_{L_3} f_s} \tag{19}$$

4.2. Selection of capacitance

Design of an appropriate capacitor for efficient energy storage and delivery, voltage regulation, filtering, decoupling, power factor correction, timing control, and satisfaction of physical constraints is critical. The value of capacitors C_1 and C_2 is depend on input current (I_{in}), switching frequency (f_s), duty ratio (D), and ripple voltage (ΔV_{C_2}) which is obtained by using (20).

$$C_1 = C_2 = \frac{I_{in}(2-D)D}{(6D-2)D\Delta V_{C_2} f_s} \tag{20}$$

The value of capacitors C_3 depend on output current (I_0), switching frequency (f_s), duty ratio (D), and ripple voltage (ΔV_{C_3}) which is obtained by using (21).

$$C_3 = \frac{I_0 D}{D\Delta V_{C_3} f_s} \tag{21}$$

5. CONTROL FLOW OF PROPOSED SMC – SIBQ DC-DC CONVERTER

The proposed SIBQ DC–DC converter employs a SMC–assisted maximum power point tracking (MPPT) mechanism to achieve high voltage gain and stable output from PV sources. The control algorithm as shown in Figure 4, begins by sensing the PV voltage and current, from which the instantaneous power is computed. This power information is compared with the reference maximum power point voltage (VMPP) to determine the direction of duty-cycle adjustment. If the PV voltage is lower than VMPP, the duty cycle is increased; otherwise, it is decreased to guide the operating point toward the MPP.

A sliding surface, defined as S=Cx-Kx, is then generated to ensure robust control under varying PV and load conditions. The controller evaluates the sliding condition S×S ̇<0 to determine system stability. When the condition is satisfied, PWM pulses are generated to drive the converter switches (S_1, S_2). If not satisfied, the control variable is adaptively corrected until the sliding criterion is met. The switching signals regulate the converter's two operation modes: Mode 1 (switches ON): The inductors L_1 and L_2 are charged through the switched-inductor network. Mode 2 (switches OFF): Stored energy is transferred through the diodes and capacitors, achieving quadratic voltage boosting. Through this dual-mode operation and SMC-based duty-cycle regulation, the converter delivers a stable high-gain DC output (e.g., 60 V) with improved dynamic response and high efficiency, even under fluctuating solar conditions.

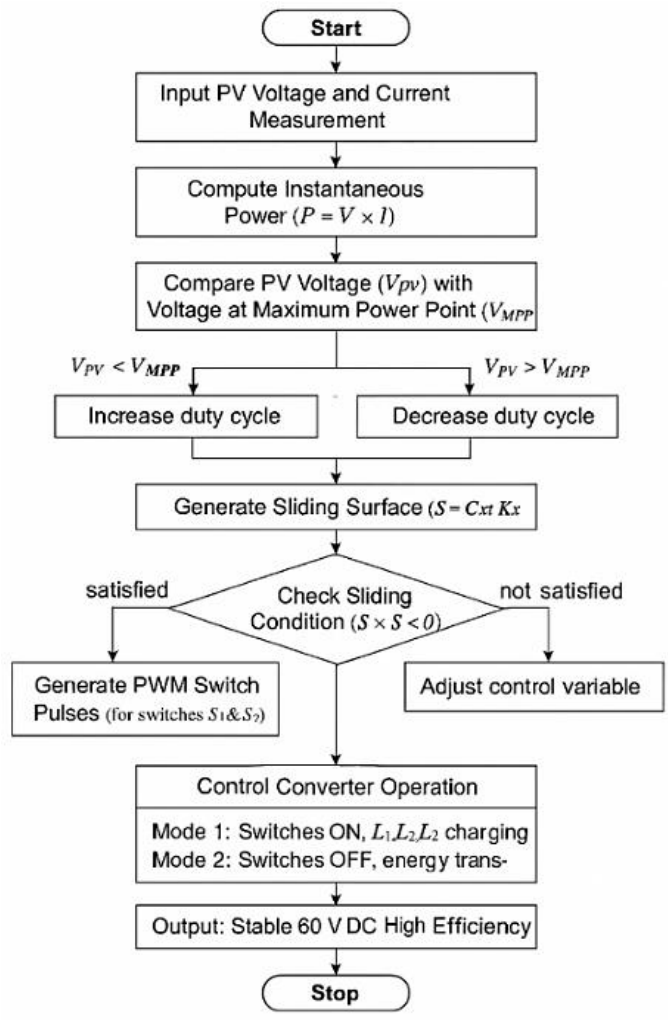

Figure 4. Sliding mode control flow for the proposed SIBQ DC-DC converter

6. RESULTS AND DISCUSSION

6.1. Closed loop analysis and testing

SMC is chosen as the control measure to maximize the power harvested from the solar energy available. This is a decision based on the fact that SMC has the inherent ability to dynamically adjust the system operating parameters to keep the system efficiently tracking variables of fluctuation in the environmental conditions. At the control loop, the SMC generator constantly produces the gated pulses of the power switches (which are known as SW1 and SW2) as shown in Figure 5.

Table 1 presents the closed-loop simulation results of the proposed converter under varying irradiance levels at a constant temperature of 25 °C. As the solar irradiance decreases from 1000 W/m² to 200 W/m², the PV voltage remains nearly constant around 12 V, indicating stable voltage regulation, while the PV current decreases proportionally with irradiance, leading to a corresponding reduction in PV power from 60 W to 11.85 W. Despite these variations, the converter maintains a high efficiency across all conditions, ranging between 91.2% and 96.2%, demonstrating its ability to effectively track the maximum power point and sustain efficient energy conversion even under low-irradiance conditions.

Figure 6 displays the battery's voltage, current, and state of charge waveform using the suggested method. In contrast to the steady decrease in current that characterizes a constant-current/constant-voltage (CC/CV) charging profile, battery voltage rises linearly with the length of charge. The converter's ability to charge and deliver a constant energy flow free from current surges and abnormalities is demonstrated by the state of charge (SOC) curve, which is distinctly linear and smooth.

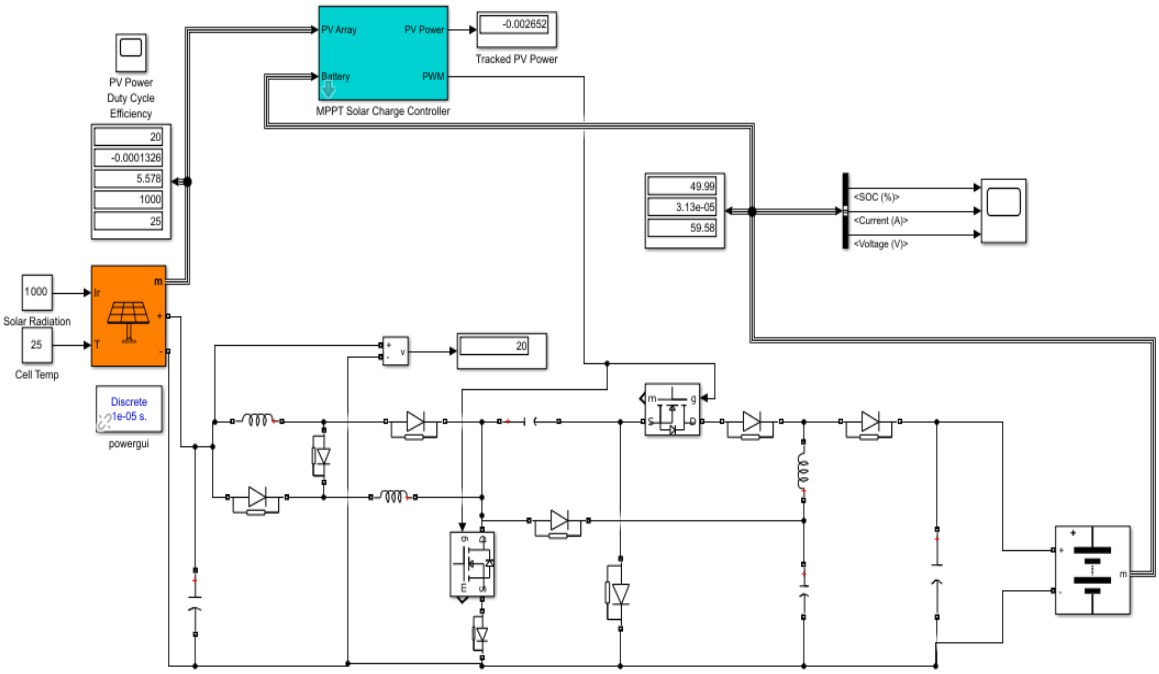

Figure 5. Closed loop modelling of a proposed SMC – SIBQ DC-DC converter

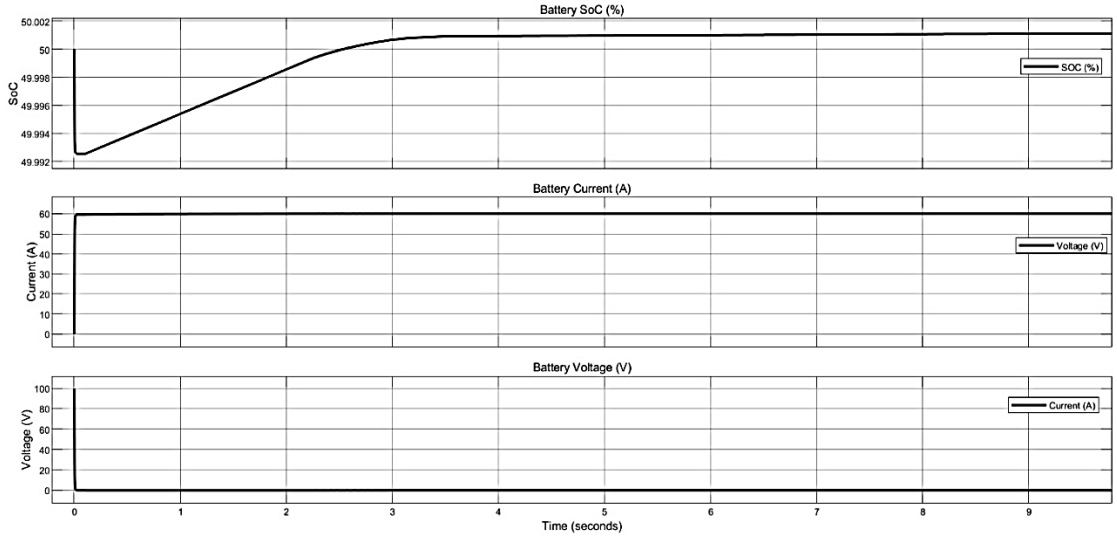

Figure 6. SMC – SIBQ DC-DC converter connected battery voltage, current, and SOC waveform

Table 1. Closed-loop simulation results of the proposed converter

Irradiance W/m^2	Temperature (°C)	PV voltage (V)	PV current (A)	PV power (W)	Output voltage (V)	Output current (A)	Output power (W)	Efficiency (%)
1000	25º	12	5	60	73	0.75	54.75	91.20
800	25º	12.07	3.98	48.04	68	0.68	46.24	96.2
600	25º	12.13	2.98	36.2	58	0.58	33.64	92.9
400	25º	12.09	1.99	24.1	48	0.48	23.04	95.6
200	25º	11.88	0.99	11.85	32	0.34	10.88	91.8

6.2. Experimental validation and testing

The experimental specifications as listed in Table 2 of the proposed system, and the MATLAB/Simulink simulation results are presented in this section. In this work, both the simulation and experimental validations were performed under identical operating conditions to ensure consistency and

reliability of the results. The converter was tested with an input voltage of 12 V DC, a target output of 60 V DC, and a switching frequency of 20 kHz. The same duty cycle ranges (0.1–0.8), and component values derived from the design equations were used in both MATLAB/Simulink simulations and the laboratory prototype. Environmental conditions such as ambient temperature (~25 °C) and load configuration (lead-acid battery as energy storage) were kept constant during testing.

As seen in Figure 7, a 60 W laboratory model was completed to validate the theoretical concepts and viability of the suggested converter. A lead-acid battery was used as the load in the prototype, which used two MOSFETs controlled by SMC under a range of environmental conditions and a 12 V DC input with a 60 V DC output voltage target. Figure 8 shows the results of the waveforms of the proposed converter SMC-SIBQ DC-DC converter, and proves that it functions in a stable and efficient way. Figure 8(a) indicates that the output voltage is constant at approximately 60 V DC, and this indicates high voltage regulation with the change of input and load conditions. Figure 8(b) shows the output current waveform, which is almost constant implying a fast transient response and low output impedance. Figures 8(c)-8(e) illustrate the voltages across the capacitors (Vc1 = 28.7 V, Vc2 = 28.7 V, Vc3 ≈ 60 V), which verify that energy is distributed correctly, the quadratic step-up gain is accurate, and also ripple is minimal, which is a good indication of energy transfer across converter stages. Figures 8(f)-8(g) indicate that the switch voltages (S_1 and S_2) are kept low (under safe limits), which confirms the low voltage stress, high reliability, and high thermal performance.

Table 2. Experimental specification

SI.No	Design of parameter	Value of parameter
A	Solar PV (input)	
1	Voc	15 V
2	Isc	5.19 A
3	V_{MPP}	12 V
4	I_{MPP}	5 A
5	Pmax	60 W
B	Load (Output)	
1	Voltage range	60 V
2	Imax	1 A
3	Pmax	60 W
C	SMC - SIBQ DC-DC converter	
1	Vin	12 VDC
2	Vout	60 VDC
3	Iin	5 A
4	I_{out}	1 A
5	dV/dt	10% of load voltage
6	dI/dt	5% of load current
7	L1	0.5 mH
8	L2	0.5 mH
9	L3	1.5 mH
10	C1	470 µF
11	C2	470 µF
12	C3	100 µF
13	Frequency	20 kHz

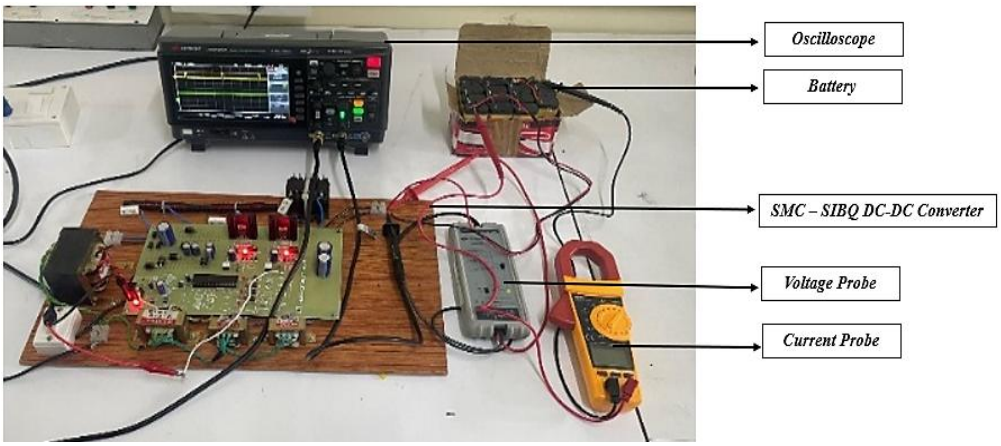

Figure 7. Experimental setup of the proposed SMC- SIBQ DC-DC converter

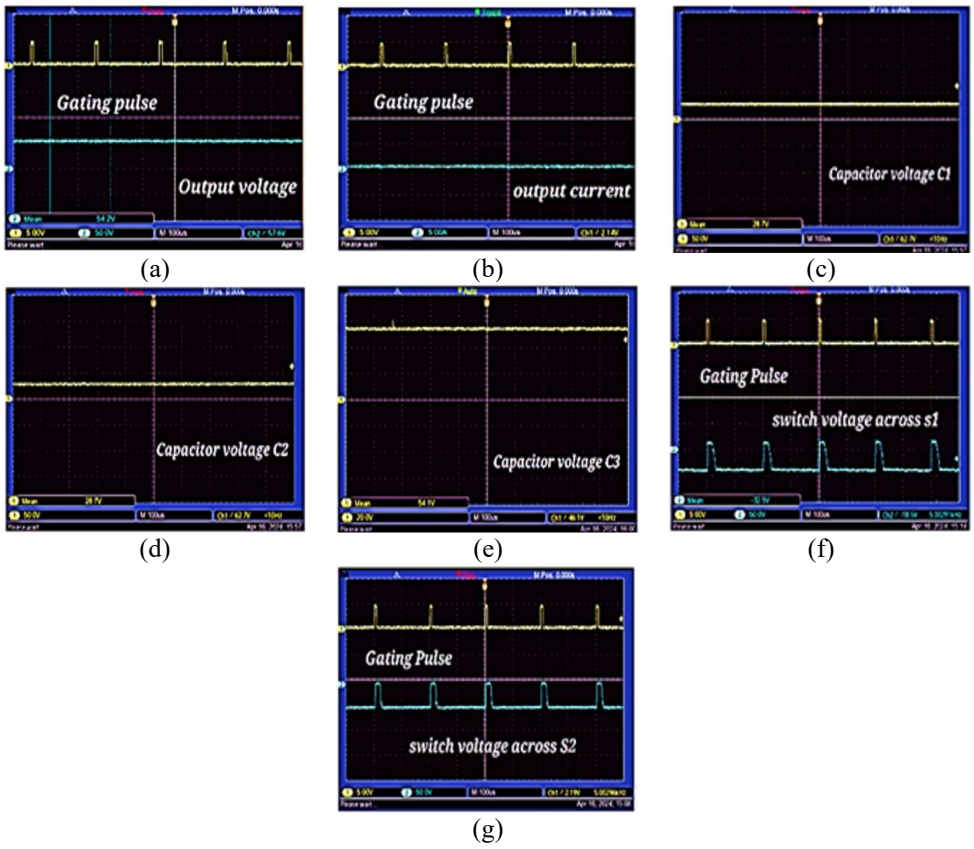

Figure 8. Experimental output waveforms obtained from the prototype hardware setup: (a) output voltage, (b) output current, (c) capacitor voltage C_1, (d) capacitor voltage C_2, (e) capacitor voltage C_3, (f) switch S_1 voltage, and (g) switch S_2 voltage

6.3. Comparative analysis

The proposed converter topology and the existing non-isolated converter topologies are compared in this section. Table 3 summarizes some of the important performance characteristics that are taken into account, including the voltage gain, component count, and voltage stress across the semiconductor device. Table 3 is a comparison of the proposed SMC-based SIBQ converter and the existing topologies in the number of components, voltage gain, and voltage stress. The proposed converter employs 14 components (2/6/3/3), and this is marginally larger than [23] and [24] but smaller than [25], a good balance between efficiency and complexity. It attains a voltage gain of $\frac{(1+D)^2}{(1-D)^2}$ that delivers much higher output to the same duty cycle. At D = 0.5 the calculated voltage gain is approximately 9x, compared to converters [23] and [25] which generate about 4x and 7x, respectively. The stress of the switch voltage is kept at $v_{in}\frac{(1+D)^2}{(1-D)^2}$, which is safe to operate, and the diode voltage stress is spread out among the components and causes little reverse recovery losses. Figure 9 provides the plot of duty ratio vs. gain of the proposed SMC – SIBQ DC-DC converter.

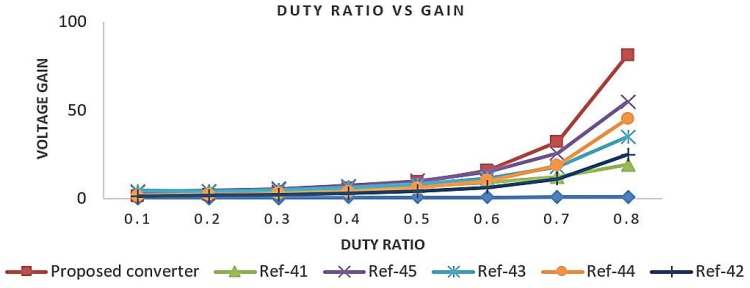

Figure 9. Proposed SMC – SIBQ DC-DC converter – duty ratio vs. gain

Table 3. Comparison of the proposed SMC - SIBQ DC-DC converter vs. existing topologies

Methods	S/D/L/C=T	Voltage gain ($\frac{v_0}{v_{in}}$)	Switch voltage stress (v_S)	Diode voltage stress(v_D)
[23]	2/2/2/2=8	$\frac{1}{(1-D)^2}$	$v_{s_1} = v_{in}\frac{1}{(1-D)}$ $v_{s_2} = v_{in}\frac{1}{(1-D)^2}$	$V_{D1} = \frac{V_{in}}{(1-D)}$ $V_{D2} = V_{in}\frac{(2-D)}{(1-D)^2}$
[24]	2/3/2/3=10	$\frac{(3-2D)}{(1-D)^2}$	$v_{s_1} = v_0\frac{(1-D)^3}{(3-2D)}$ $v_{s_2} = v_0\frac{(1-2D(1-D)^3)}{(3-2D)}$	Not mentioned
[25]	2/7/4/3=16	$\frac{(3+D)}{(1-D)}$	$v_{s_1} = v_0\frac{2}{(3+D)}$ $v_{s_1} = v_0\frac{(1+D)}{(3+D)}$	$V_{D1} = V_{D2} = \frac{(5D-1)}{(3+D)}V_o$ $V_{D3} = \frac{(11D-3)}{(3+D)}V_o$ $V_{D4} = \frac{(1-D)}{(3+D)}V_o$ $V_{D5} = V_{D6} = \frac{(5D-1)}{(3+D)}V_o$ $V_{D7} = V_{Do}$
Proposed	2/6/3/3=14	$\frac{(1+D)^2}{(1-D)^2}$	$v_{s_1} = v_{in}\frac{(1+D)^2}{(1-D)^2}$ $v_{s_2} = v_{in}\frac{(1+D)^2}{(1-D)^2}$	$v_{D_3} = v_{D_1} = v_{D_2} = v_0\frac{(1-D)^2}{(1+D)^2}$ $v_{D_4} = v_{D_5} = v_{in}\frac{(1+D)}{(1-D)}$ $v_{D_6} = \frac{3(1+D)}{(1-D)}$

6.4. Discussion

The effectiveness of the proposed SMC-SIBQ DC-DC converter, certain internal and external threats may influence the validity of these outcomes. Internally, the accuracy of component parameter modeling, measurement tolerances, and idealized switching assumptions in MATLAB/Simulink may lead to minor deviations between simulated and real-time performance. Furthermore, environmental variations such as temperature fluctuations, parasitic losses, and unmodeled electromagnetic interference can affect system stability during experimental validation. Externally, the test setup was performed under controlled laboratory conditions that may not fully replicate large-scale or dynamic field environments in electric vehicle charging infrastructures. Additionally, hardware limitations and prototype scaling may influence converter efficiency when integrated with high-power EV systems. Future work will therefore focus on extensive real-world testing and long-term operational analysis to further strengthen the robustness and generalizability of the presented results.

7. CONCLUSION

In this research, a non-isolated switched inductor quadratic DC-DC converter is proposed based on SMC. The suggested approach is optimal for charging electric vehicles and an application related to renewable energy, as it aims to optimize efficiency and gain considerable voltage. Sliding mode control strategy is used to make the system more robust to the changes in parametric values to make it a stable and efficient system under different load conditions and extract power in the most efficient way when charging is done by renewable means. The solution is proposed and allows exploiting step-up continuous conduction mode, which minimizes switching losses and enhances thermal balance, which are major issues in high-power applications. The effectiveness of the proposed converter is confirmed with the help of MATLAB/Simulink simulations and experimental results of a lab prototype.

ACKNOWLEDGMENTS

The authors extend their sincere gratitude to the MSEC EEE, 2024 batch UG project students—Hariharan M, Jawahar KS, and Liyakathali M, for their significant contributions that helped achieve meaningful results in this research. The authors also acknowledge the Management, the Principal, the Department of EEE, and the National Solar Electric Vehicle Team Workstation at Mepco Schlenk Engineering College, Sivakasi, for their continuous encouragement and support throughout the course of this work.

FUNDING INFORMATION

Authors state no funding involved.

AUTHOR CONTRIBUTIONS STATEMENT

This journal uses the Contributor Roles Taxonomy (CRediT) to recognize individual author contributions, reduce authorship disputes, and facilitate collaboration.

Name of Author	C	M	So	Va	Fo	I	R	D	O	E	Vi	Su	P	Fu
Jawahar Marimuthu	✓	✓	✓		✓	✓	✓	✓	✓	✓	✓		✓	
Edward Rajan Samuel Nadar		✓		✓	✓	✓			✓	✓		✓		

C : **C**onceptualization
M : **M**ethodology
So : **So**ftware
Va : **Va**lidation
Fo : **Fo**rmal analysis
I : **I**nvestigation
R : **R**esources
D : **D**ata Curation
O : Writing - **O**riginal Draft
E : Writing - Review & **E**diting
Vi : **Vi**sualization
Su : **Su**pervision
P : **P**roject administration
Fu : **Fu**nding acquisition

CONFLICT OF INTEREST STATEMENT

The authors declare that they have no known competing financial interests or personal relationships that could have appeared to influence the work reported in this paper.

DATA AVAILABILITY

Data sharing not applicable to this article as no datasets were generated or analyzed during the current study.

REFERENCES

[1] I. Ahmed, M. Adnan, M. Ali, and G. Kaddoum, "Supertwisting sliding mode controller for grid-to-vehicle and vehicle-to-grid battery electric vehicle charger," *Journal of Energy Storage*, vol. 70, p. 107914, Oct. 2023, doi: 10.1016/j.est.2023.107914.

[2] R. Sabzehgar, Y. M. Roshan, and P. Fajri, "Modelling and sliding-mode control of a single-phase single-stage converter with application to plug-in electric vehicles," *IET Power Electronics*, vol. 12, no. 3, pp. 620–626, Mar. 2019, doi: 10.1049/iet-pel.2018.5664.

[3] S. Singh, S. K. Soni, K. A. Singh, and R. K. Saket, "Sliding mode control for bidirectional DC-DC power converter in electric vehicle charger for G2V and V2G applications," in *2023 IEEE 3rd International Conference on Sustainable Energy and Future Electric Transportation (SEFET)*, IEEE, Aug. 2023, pp. 1–6, doi: 10.1109/SeFeT57834.2023.10245726.

[4] R. Tiwari, K. Kumar, N. R. Babu, and K. R. Prabhu, "Coordinated MPPT and DPC strategies for PMSG based grid connected wind energy conversion system," *Energy Procedia*, vol. 145, pp. 339–344, Jul. 2018, doi: 10.1016/j.egypro.2018.04.061.

[5] P. Upadhyay and R. Kumar, "A ZVS-ZCS quadratic boost converter to utilize the energy of PV irrigation system for electric vehicle charging application," *Solar Energy*, vol. 206, pp. 106–119, 2020, doi: 10.1016/j.solener.2020.05.068.

[6] S. Bairabathina and S. Balamurugan, "Review on non-isolated multi-input step-up converters for grid-independent hybrid electric vehicles," *International Journal of Hydrogen Energy*, vol. 45, no. 41, pp. 21687–21713, 2020, doi: 10.1016/j.ijhydene.2020.05.277.

[7] A. Masoud, M. Packnezhad, and H. Farzanehfard, "A single-switch ultra-high step-up DC-DC converter with low voltage stress based on quadratic y-sources topology," in *2023 14th Power Electronics, Drive Systems, and Technologies Conference, PEDSTC 2023*, 2023, doi: 10.1109/PEDSTC57673.2023.10087094.

[8] M. Suthar, U. B. Manthati, C. R. Arunkumar, P. Srinivas, F. Alsaif, and I. Zaitsev, "Enhancing electric vehicle performance with a hybrid PI-sliding mode controller for battery supercapacitor integration," *International Journal of Energy Research*, vol. 2024, 2024, doi: 10.1155/2024/1105301.

[9] J. G. Malar, V. Thiyagarajan, N. B. M. Selvan, and M. D. Raj, "Electric vehicle onboard charging via Harris Hawks optimization-based fractional-order sliding mode controller," *Revue Roumaine des Sciences Techniques Serie Electrotechnique et Energetique*, vol. 68, no. 1, pp. 30–35, 2023, doi: 10.59277/rrst-ee.2023.68.1.5.

[10] J. Ding, S. Zhao, S. Gao, and H. Yin, "A single-switch high step-up DC-DC converter based on three-winding coupled inductor and pump capacitor unit," *IEEE Transactions on Power Electronics*, vol. 37, no. 3, pp. 3053–3061, 2022, doi: 10.1109/TPEL.2021.3113255.

[11] S. Bagherwal and S. Mahapatra, "A robust sliding mode control strategy for DC voltage stabilization in solar powered electric vehicle charging station," *International Journal of Green Energy*, vol. 22, no. 2, pp. 432–448, 2025, doi: 10.1080/15435075.2024.2415542.

[12] S. Habibi, R. Rahimi, M. Ferdowsi, and P. Shamsi, "Coupled inductor-based single-switch quadratic high step-up DC-DC converters with reduced voltage stress on switch," *IEEE Journal of Emerging and Selected Topics in Industrial Electronics*, vol. 4, no. 2, pp. 434–446, 2023, doi: 10.1109/JESTIE.2022.3209146.

[13] P. Deepa, S. Rajakumar, P. J. Shermila, E. A. Devi, M. E. Prince, and A. J. G. Malar, "New hybrid Cuk-Landsman high gain dc-dc converter modelling and analysis," *SSRG International Journal of Electrical and Electronics Engineering*, vol. 9, no. 8, pp. 8–16, 2022, doi: 10.14445/23488379/IJEEE-V9I8P102.

[14] M. Zaid *et al.*, "A family of transformerless quadratic boost high gain DC-DC converters," *Energies*, vol. 14, no. 14, 2021, doi: 10.3390/en14144372.

[15] H. Gholizadeh, R. S. Shahrivar, M. R. Hashemi, E. Afjei, and S. A. Gorji, "Design and implementation a single-switch step-up DC-DC converter based on cascaded boost and Luo converters," *Energies*, vol. 14, no. 12, 2021, doi: 10.3390/en14123584.

[16] A. M. Mohammed, S. N. H. Alalwan, A. Taşcıkaraoğlu, and J. P. S. Catalão, "Sliding mode-based control of an electric vehicle fast charging station in a DC microgrid," *Sustainable Energy, Grids and Networks*, vol. 32, 2022, doi: 10.1016/j.segan.2022.100820.
[17] D. Mazumdar, P. K. Biswas, C. Sain, and T. S. Ustun, "GAO optimized sliding mode based reconfigurable step size PB&O MPPT controller with grid integrated EV charging station," *IEEE Access*, vol. 12, pp. 10608–10620, 2024, doi: 10.1109/ACCESS.2023.3344275.
[18] R. Huang, F. Hong, and D. Ghaderi, "Sliding mode controller-based e-bike charging station for photovoltaic applications," *International Transactions on Electrical Energy Systems*, vol. 30, no. 4, 2020, doi: 10.1002/2050-7038.12300.
[19] K. Mathew K and D. M. Abraham, "Particle swarm optimization-based sliding mode controllers for electric vehicle onboard charger," *Computers and Electrical Engineering*, vol. 96, 2021, doi: 10.1016/j.compeleceng.2021.107502.
[20] S. Y. Rahme, S. Islam, S. M. Amrr, A. Iqbal, I. Khan, and M. Marzband, "Adaptive sliding mode control for instability compensation in DC microgrids due to EV charging infrastructure," *Sustainable Energy, Grids and Networks*, vol. 35, 2023, doi: 10.1016/j.segan.2023.101119.
[21] S. Valedsaravi, K. Mandal, A. El Aroudi, and L. Martínez-Salamero, "Digital sliding mode control of a 3-phase ac-dc rectifier for ultra-fast charging of EV battery," *IFAC-PapersOnLine*, vol. 58, no. 13, pp. 430–435, 2024, doi: 10.1016/j.ifacol.2024.07.520.
[22] A. D. Falehi, "MOSFSA-based CFBHSMC to enhance control accuracy and robustness of proton exchange membrane fuel cell," *Cleaner Chemical Engineering*, vol. 11, 2025, doi: 10.1016/j.clce.2025.100168.
[23] A. D. Falehi and E. Salary, "An innovative high-gain multi-stage non-isolated step-up converter controlled by optimal interval type-2 fuzzy system based maximum power point tracking," *Results in Engineering*, vol. 24, 2024, doi: 10.1016/j.rineng.2024.103458.
[24] A. D. Falehi, "Optimal power tracking of DFIG-based wind turbine using MOGWO-based fractional-order sliding mode controller," *Journal of Solar Energy Engineering*, vol. 142, no. 3, Jun. 2020, doi: 10.1115/1.4044977.
[25] A. D. Falehi, "An innovative optimal RPO-FOSMC based on multi-objective grasshopper optimization algorithm for DFIG-based wind turbine to augment MPPT and FRT capabilities," *Chaos, Solitons & Fractals*, vol. 130, p. 109407, Jan. 2020, doi: 10.1016/j.chaos.2019.109407.

BIOGRAPHIES OF AUTHORS

Jawahar Marimuthu received the B.E. (EEE), M.E. (power electronics and drives) from the Faculty of Electrical Engineering, Anna University, Chennai, in 2012 and 2016, respectively. He has been pursuing his Ph.D. (electrical engineering) from the Centre for Research, Anna University, Chennai, since 2021. He is currently an assistant professor (senior grade) in the Department of Electrical and Electronics Engineering at Mepco Schlenk Engineering College, Sivakasi. His research interest includes power electronics and drives and soft-computing techniques. He was a recipient of summer faculty fellowship from IIT Delhi in 2017. He is the life member of ISTE and member of IAENG. He can be contacted at email: jawahar.m@mepcoeng.ac.in.

Edward Rajan Samuel Nadar received the B.E. (ICE) from the Faculty of Electrical Engineering, Madurai Kamaraj University, Madurai in 1991, M.E. (electrical engineering) from the Faculty of Electrical Engineering, Jadavpur University, Kolkata in 1996, and Ph.D. (electrical engineering) from the Faculty of Electrical Engineering, Madurai Kamaraj University, Madurai, in 2006. He is currently a senior professor in the Department of Electrical and Electronics Engineering, Mepco Schlenk Engineering College, Sivakasi. His research interests include renewable power generation, power converters, modelling and simulation of instrumentation systems, medical image processing, and biomedical instrumentation. He is the life member of ISTE, a member of IAENG, fellow of the Institution of Engineers (India). He can be contacted at email: sedward@mepcoeng.ac.in.